Remote Atmospheric Pressure Infrared Matrix-Assisted Laser Desorption-Ionization Mass Spectrometry (Remote IR-MALDI MS) of Proteins

Benoit Fatou, Michael Ziskind, Philippe Saudemont, Jusal Quanico, Cristian Focsa, Michel Salzet, Isabelle Fournier

Remote Atmospheric Pressure Infrared Matrix-Assisted Laser Desorption-Ionization Mass Spectrometry (Remote IR-MALDI MS) of Proteins*[S]

Benoit Fatou‡§, Michael Ziskind§, Philippe Saudemont‡¶, Jusal Quanico‡§, Cristian Focsa§, Michel Salzet‡, and Isabelle Fournier‡‖

Remote Infrared Matrix-Assisted Laser Desorption/Ionization (Remote IR-MALDI) system using tissue endogenous water as matrix was shown to enable *in vivo* real-time mass spectrometry analysis with minimal invasiveness. Initially the system was used to detect metabolites and lipids. Here, we demonstrate its capability to detect and analyze peptides and proteins. Very interestingly, the corresponding mass spectra show ESI-like charge state distribution, opening many applications for structural elucidation to be performed in real-time by Top-Down strategy. The charge states show no dependence toward laser wavelength or length of the transfer tube. Indeed, remote analysis can be performed 5 m away from the mass spectrometer without modification of spectra. On the contrary, addition of glycerol to water shift the charge state distributions toward even higher charge states. The desorption/ionization process is very soft, allowing to maintain protein conformation as in ESI. Observation of proteins and similar spectral features on tissue, when protein standards are deposited on raw tissue pieces, could potentially open the way to their direct analysis from biological samples. This also brings interesting features that could contribute to the understanding of IR MALDI ionization mechanism. ***Molecular & Cellular Proteomics 17: 10.1074/mcp.TIR117.000582, 1637–1649, 2018.***

The last decade technological developments have pushed the progressive translation of mass spectrometry (MS) from static analysis of extracted molecules to their possible examination in the *in situ* context. This is clearly illustrated by the dynamics in the field related to the development of ambient ionization mass spectrometry (AIMS)[1] methods over the past 10 years. AIMS methods allow the detection and identification of molecules from native samples at atmospheric pressure (AP) and room temperature (RT) with little or no sample preparation. More than thirty ambient ionization sources are described in literature (1–5) for the sampling of surfaces, liquids and gases. For surfaces, various concepts and principles have been proposed to obtain ion production including for example the use of solvent spray, gas flow (6, 7), plasma (8, 9) or laser (10, 11). The importance of the field of applications and the many researches in which *in situ* analysis can be useful have further promoted the development of methods for real-time and *in vivo* analysis. Real-time *in vivo* analysis requires pushing further the limits of technologies because many of the already developed methods cannot be applied to the *in vivo* context or are restricted to a limited number of applications. Looking for *in vivo* real-time devices with broad range applicability is a real challenge that might require the ion production process to be decoupled from the mass analyzer and placed remotely with a transport of the ions over few meters of distances. This was shown to be possible by the group of Takats with the Rapid Evaporative Ionization Mass Spectrometry (REIMS) technology (iKnife device), a system for real-time analysis under intraoperative conditions of patients undergoing cancer surgery (12). In the iKnife, ions liberated in the smoke produced by the electric scalpel while the surgeon is cutting a patient's tissue are analyzed in real-time (13) to give access to molecular signatures that can be used to diagnose if the tissue is diseased or not.

Recently we have demonstrated that *in vivo* real-time analysis can also be performed with lesser invasiveness by laser ablation using the SpiderMass instrument (14). Ions can be produced by irradiating tissues with nanosecond pulses of a mid-IR laser tuned at 2.94 μm, in resonance with the optical absorption peak of water (O-H stretching mode). These can then be transported over a few meters to the MS instrument for analysis without requiring any post-ionization (14). With this system we have demonstrated that the water content of

From the ‡Université de Lille, INSERM, U1192 - Laboratoire Protéomique, Réponse Inflammatoire et Spectrométrie de Masse (PRISM), F-59000 Lille, France; §Université de Lille, CNRS, UMR 8523 - PhLAM - Physique des Lasers Atomes et Molécules, F-59000 Lille, France; ¶SATT Nord, Immeuble Central Gare, 4e étage, 25, Avenue Charles St Venant, F-59800 Lille, France

Received December 30, 2017, and in revised form, April 12, 2018
Published, MCP Papers in Press, April 13, 2018, DOI 10.1074/mcp.TIR117.000582

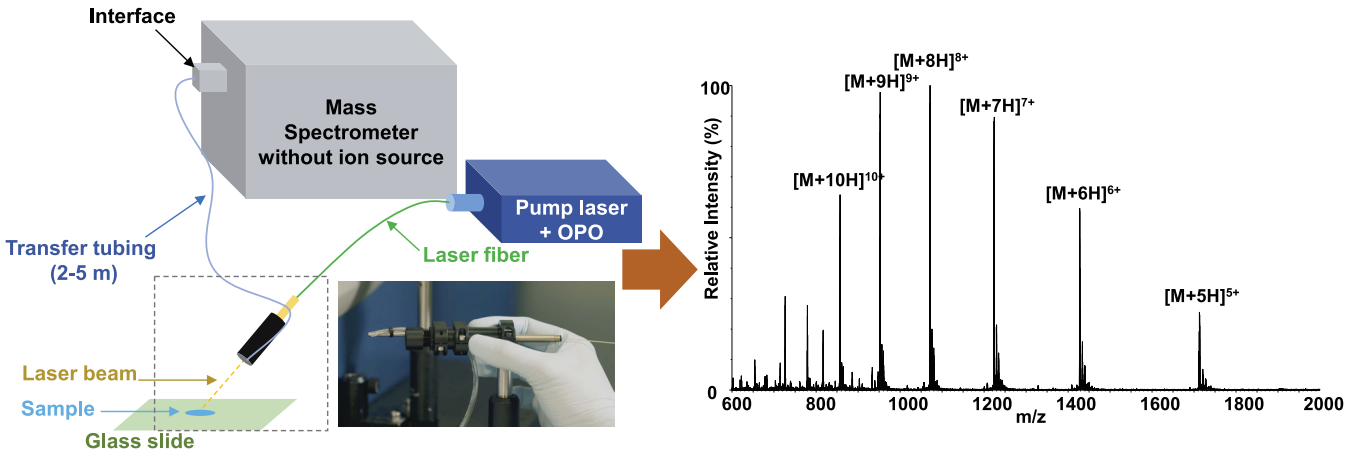

FIG. 1. **Schematic representation of the Remote IR-MALDI prototype so-called SpiderMass system.** The system is composed of three parts including a fibered laser tuned to 2.94 μm equipped with a hand-piece for maneuvering the laser beam onto surfaces, a Tygon® ND 100–65 transfer tubing line connected to the laser hand-piece on one end and to the inlet of the MS instrument on the other, and the MS instrument itself (here an Ion mobility QqTOF).

biological tissues can be advantageously used for MS analysis without addition of any external matrix molecule. Because in these conditions the ablation depth is limited to a few micrometers per laser shot, it is possible to perform *in vivo* analysis on human skin with low invasiveness. The collective effects and the low extent of fragmentation observed during these experiments suggest an IR-MALDI mechanism with water as the natural endogenous MALDI matrix. Because water is absorbing at the laser wavelength and is in large excess compared with the analytes, it indeed possesses the characteristics of a MALDI matrix. In initial experiments we have shown that specific metabolite and lipid molecular signatures could be retrieved from different tissues and different cell phenotypes.

In the present study we evaluate the potential of this remote atmospheric pressure Infrared MALDI system (Fig. 1) in analyzing peptides and proteins because *in vivo* real-time proteomics is a clear challenge with high impact applications. Interestingly, our first experiments using standard peptides and proteins have revealed the presence of multiply charged ions with spectral profiles very similar to those obtained by electrospray ionization (ESI). This was rather unexpected considering the long transfer line (2 meters) for transporting ions from the laser microprobe to the interface of the MS analyzer. We therefore studied the different parameters that could play a role in the observation of these species to understand the underlying mechanisms leading to the formation of these multiply charged ions.

EXPERIMENTAL PROCEDURES

Experimental Design and Statistical Rationale—We performed the experiments with a novel prototype of the SpiderMass instrument already described in a previous study (14). Ions are generated remotely from the MS instrument and transported in real-time to the MS analyzer. Ion production is promoted by Resonant Infrared Laser Ablation (RIR-LA) based on the highly effective excitation of O-H bonds in water molecules naturally present in most biological samples allowing for the MALDI process to occur. Peptide and protein standards are analyzed using SpiderMass to study the influence of various parameters, including laser wavelength, transfer tube length and temperature, or solution pH, and assess the potential of the system for Top Down analysis. Each sample is prepared in triplicate and analyzed at least three times.

Sample Preparation—Water (H_2O) and isopropanol were purchased from Biosolve (Dieuze, France). The protein mix was purchased from Bruker Daltonics (Bremen, Germany). Angiotensin I, bovine ubiquitin, cytochrome *c* from horse heart, chicken lysozyme, trifluoroacetic acid (TFA) and glycerol were purchased from Sigma Aldrich (Saint-Quentin Fallavier, France).

For most of the experiments, the two analytes (angiotensin-I and bovine ubiquitin) were first prepared at a concentration of 10^{-3} M in water. This solution was further diluted in glycerol/water (1:1; v/v), water or 0.2% TFA in water to obtain a final concentration of 500 μM. For each experiment, 2 μl of the working solution were deposited onto a glass slide just before SpiderMass analysis. For the protein standard mix, an equal volume of the solution was added to glycerol and 2 μl of this sample was deposited onto a glass slide and samples were spotted in triplicate. For sensitivity tests, the stock solution was further diluted 10-, 100-, and 1000-fold to achieve the targeted concentration but sample deposition was kept the same. Lowest tested concentration was 250 fmoles/μl for each analyte but this was not the Limit of detection (LOD).

For the pH experiments, the glycerol/water solutions with pH adjusted to 3, 5, 7 and 9 were first prepared. The glycerol/water solution is at pH = 5. Thus, for pH < 5, pH was adjusted by adding an appropriate volume of HCl (1 M) and for pH > 5 by adding an appropriate volume of NaOH (0.1 M). Then, 20 μl of the analytes

[1] The abbreviations used are: AIMS, ambient ionization mass spectrometry; IR, infrared; MALDI, matrix-assisted laser; esorption/ionization; AP, atmospheric pressure; RT, room temperature; REIMS, rapid evaporative ionization mass spectrometry; Re, remote; ESI, electrospray ionization; OPO, optical parametric oscillator; RIR-LA, resonant infrared laser ablation; TFA, trifluoroacetic acid; SAII, solvent-assisted ionization inlet; MAII, matrix-assisted ionization inlet; MS/MS or MS^2, tandem mass spectrometry; CID, collision-induced dissociation; PSD, post-source decay; LOD, limit of detection.

(ubiquitin, lysozyme, or cytochrome C) suspended at 500 μM in pure water were dried in speedvac (ThermoScientific, Waltham, MA) and resuspended in 20 μl of the pH-adjusted glycerol/water solution (1:1; v/v). Then 2 μl of the final solution was deposited onto a glass slide for SpiderMass analysis.

For *in situ* protein analysis, 100 μl of a protein mix containing ubiquitin, lysozyme, and cytochrome C (suspended at 500 μM each in pure H_2O) were dried in speedvac and resuspended in 100 μl of a solution of IPA/Glycerol (1:1; v/v). 2.5 μl of this solution was deposited onto a raw piece of food grade beef liver tissue bought from a local store and analyzed by SpiderMass after the droplet was adsorbed by the tissue.

Instrumentation—The basic design of the so-called SpiderMass Remote IR-MALDI instrument setup is already described in a previous study (14). In these experiments, the prototype was equipped with a fibered infrared Optical Parametric Oscillator (OPO) system tunable at wavelengths between 2.8 μm to 3.1 μm (Radiant version 1.0.1, OPOTEK Inc., Carlsbad, CA) pumped by 1.064 μm radiation delivered by a Q-switched 10-ns pulse width Nd:YAG laser (Quantel Laser, Les Ulis, France). A 1-m biocompatible laser fiber with 450 μm inner diameter (ID)(HP fiber, Infrared Fiber Systems, Silver Spring, MD) was connected to the exit of the OPO system and focused by a 20 mm focal length CaF_2 lens attached at its end leading to a 400 μm spot size. A Tygon® ND 100–65 tubing (2.4 mm ID, 4 mm outer diameter, Akron, OH) was used to aspirate the ablated material and was directly connected to the inlet of the mass spectrometer (Synapt G2s, Waters Corporation, Manchester, United Kingdom) through a modified atmospheric pressure interface described elsewhere (15) (Fig. 1). The interface includes a kanthal heated coil which was set at 7.5 W (i = 3 A and U = 2.5V).

The samples were measured by simply irradiating the deposited droplet or the tissue sample over 5 s irradiation periods at 1.6 J/cm^2. The fluence was decreased to 0.8 J/cm^2 when the wavelength was tuned to keep it constant over the screened range. Spectral acquisition was performed in positive resolution mode with a scan time of 0.5 s. For MS/MS experiments spectra were recorded in real-time conditions for angiotensin I and ubiquitin by subjecting the parent ions to collision-induced dissociation (CID) in the transfer cell using 20 and 35 V RF voltages, respectively. For experiments related to the evaluation of the transfer tube temperature, a flexible heating cable system (isopad T7000, Thermocoax, Suresnes, France) was uniformly winded around the aspiration tube.

Data Processing—Each acquisition was performed in triplicate. The recorded MS spectra were processed using MassLynx V4.1 (SCN833, Waters Corporation). Averaged MS spectra were extracted from the total ion chromatogram by averaging all the spectra recorded over the 5-s laser irradiation period which corresponds to a total of 50 laser shots, with the laser having a 10Hz repetition rate. Peak area was calculated by integrating the signal of the protonated ions of the analyte including all the isotopes. Because cationized ions were not observed in all experiments, they were not taken into account for measuring signal intensity. The MS/MS spectra were exported to mMass software v5.5 (16) for labeling of fragment ions according to the expected theoretical fragmentation of the standards.

RESULTS

Mass Spectra of Angiotensin I (MW_{mono} = 1295.67 u.) and bovine ubiquitin (MW_{mono} = 8559.61 u.) prepared under different conditions and recorded in real-time using a 2-m long transfer line over 5 s laser irradiation (1.6 J/cm^2) periods are presented in Fig. 2 and supplemental Fig. S1. Multiply charged ion distributions similar to an "ESI-like" charge state distribution are observed for both compounds without any post-ionization. Comparing different preparations shows a clear evolution of the charge state (z) distribution (supplemental Fig. S1). For angiotensin I that is left to dry on the plate, only singly charged ions are observed. Signal observed for dried angiotensin I could be attributed to the presence of residual water molecules trapped in the dried spot as previously suggested by Talrose and collaborators (19). Signal from dried angiotensin I could as well originate from direct absorption of the photons by the peptide which then could explain why only singly charged ions are observed. When angiotensin I is analyzed in water, doubly charged ions are detected. Using water/glycerol (1:1, v/v) as matrix (20–22), the most intense signal becomes the $[M+2H]^{2+}$ ion, and even $[M+3H]^{3+}$ is observed. It can also be noticed that the presence of glycerol limits salt adduct formation compared when angiotensin I was analyzed in water or as a dried spot. For ubiquitin a similar trend is observed. In water, ubiquitin presents a charge state distribution up to z = 11, with maximum at z = 7. In glycerol/water, the maximum of the distribution is shifted to z = 9 and the maximum charge state observed is z = 12. No signal could be recorded for dried ubiquitin. Comparison to previously obtained results in IR AP-MALDI by Laiko *et al.* (23) or by König *et al.* (24) using glycerol/water mixture or water as matrix shows that higher charge states are observed here (previously limited to z = 2 for glycerol/water in these studies). The observed distribution for ubiquitin is very similar to what was previously observed by Trimpin and coll (25). in their ambient ionization methods such as solvent assisted ionization inlet (SAII) or matrix assisted ionization inlet (MAII) (25). Charge state distribution is not affected by the concentration of the sample. As low as 250 fmol/μl of sample could be analyzed for all analytes tested, using 50 laser shots (5s irradiation period) on 2 μl of sample for a total of 500 fmoles spotted, without any significant decrease in signal intensity as shown in supplemental Figs. S2–S4. This means that the system can operate on sample quantities in a range useful for biological applications with an LOD below these tested values.

Real-time analysis of a protein mixture composed of insulin (MW 5805 u.), ubiquitin, myoglobin (MW 17184 u.) and cytochrome C (MW 12327 u.), using glycerol/water as matrix is shown Fig. 3. Each protein presents a charge state distribution close to what would be expected for ESI. For example $[M+15H]^{15+}$ ion of myoglobin and $[M+19H]^{19+}$ ion of cytochrome C are detected. Identification of proteins is a central problematic in proteomics. Using the Remote IR-MALDI system we can identify peptides and proteins by MS^2 performed under real-time conditions. Because high charge state ions are generated, good fragmentation yields can be obtained even though the MS instrument itself operates with CID under low collision energy conditions. For angiotensin I, MS^2 was performed on the doubly charged $[M+2H]^{2+}$ ion (supplemental Fig. S5). Most of daughter ions of the b_i^+ and y_i^+ series as

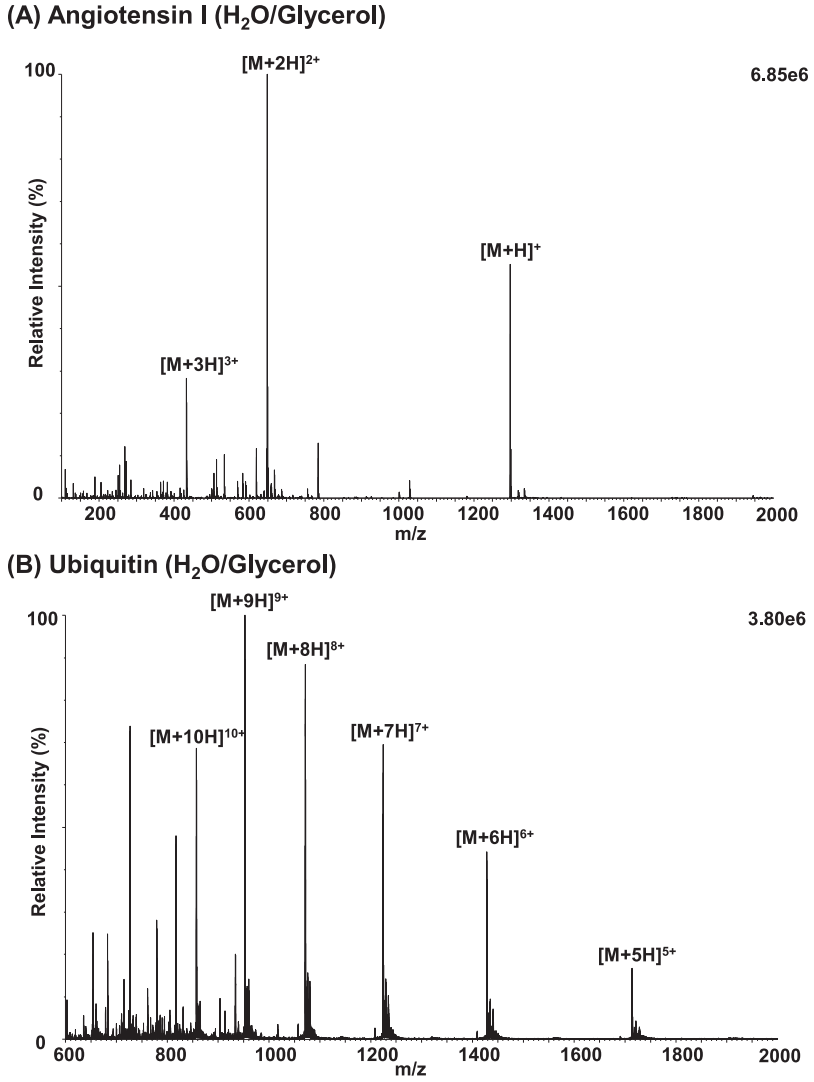

FIG. 2. **MS spectra recorded in positive mode using the Re-AP-IR-MALDI system for (*A*) angiotensin-I and (*B*) bovine ubiquitin in water/glycerol (1:1, v/v) as matrix.** 2 μl of analyte at 5×10^{-4} M was deposited onto a glass slide and submitted to 5 s laser irradiation period (ca. 50 laser shots).

well as few ions of the a_i^+ series are observed, making a clear assignment of angiotensin I (supplemental Fig. S5*B*). For ubiquitin, because of the large charge state distribution, several ions can be used for structural elucidation. Fig. 4 shows examples of the fragmentation of the $[M+7H]^{7+}$ and $[M+8H]^{8+}$ ions of ubiquitin. Again b_i^+ and y_i^+ fragmentation series are largely represented and offer sequence coverage allowing for unambiguous identification of bovine ubiquitin by the Top-Down approach under real-time conditions.

To better understand the ion formation mechanism leading to the observation of these multiply charged ions, different parameters of the system were evaluated. We first investigated the laser wavelength by scanning with the OPO in the range of 2.8–3.1 μm with 25-step increments at 0.8 J/cm^2. MS spectra recorded for angiotensin I and ubiquitin are presented in supplemental Fig. S6 and supplemental Fig. S7 respectively. We observe a notable resonance phenomenon with maximum intensity of the ion signals around 2.9–3.0 μm for the two analytes. This is expected because both water and glycerol show a strong and large absorption band in this range. We observe a similar behavior for both the analytes (supplemental Fig. S8) and the matrix (supplemental Fig. S9) as demonstrated by the evolution of the intensity of the ion signals of glycerol itself. If the total signal intensity is affected by the laser wavelength, the relative intensity of the signals remains unmodified, charge state being unchanged. This collective behavior is typical of a MALDI process as observed for vacuum UV-MALDI (26).

We then investigated how the transfer tube length can affect the MS spectra and ion rates. Indeed, in the specific configuration of SpiderMass the ions are transmitted over long distances by simple ambient aspiration. One can wonder

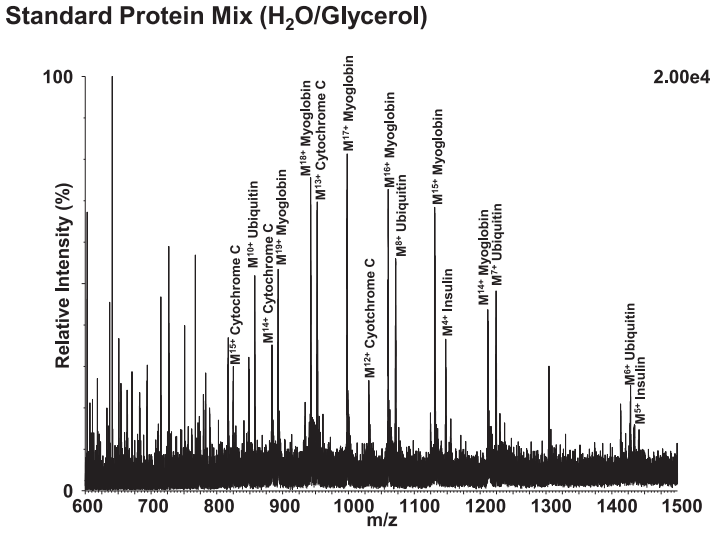

FIG. 3. **MS spectrum recorded in positive mode using the Re-AP-IR-MALDI system of a standard protein mix composed of bovine Insulin, bovine ubiquitin, cytochrome, C and myoglobin and prepared with glycerol/water (1:1, v/v) as matrix.** 2 μl of standard protein mix was deposited onto a glass slide after dilution by a factor of 2 and submitted to 5 s laser irradiation period (ca. 50 laser shots).

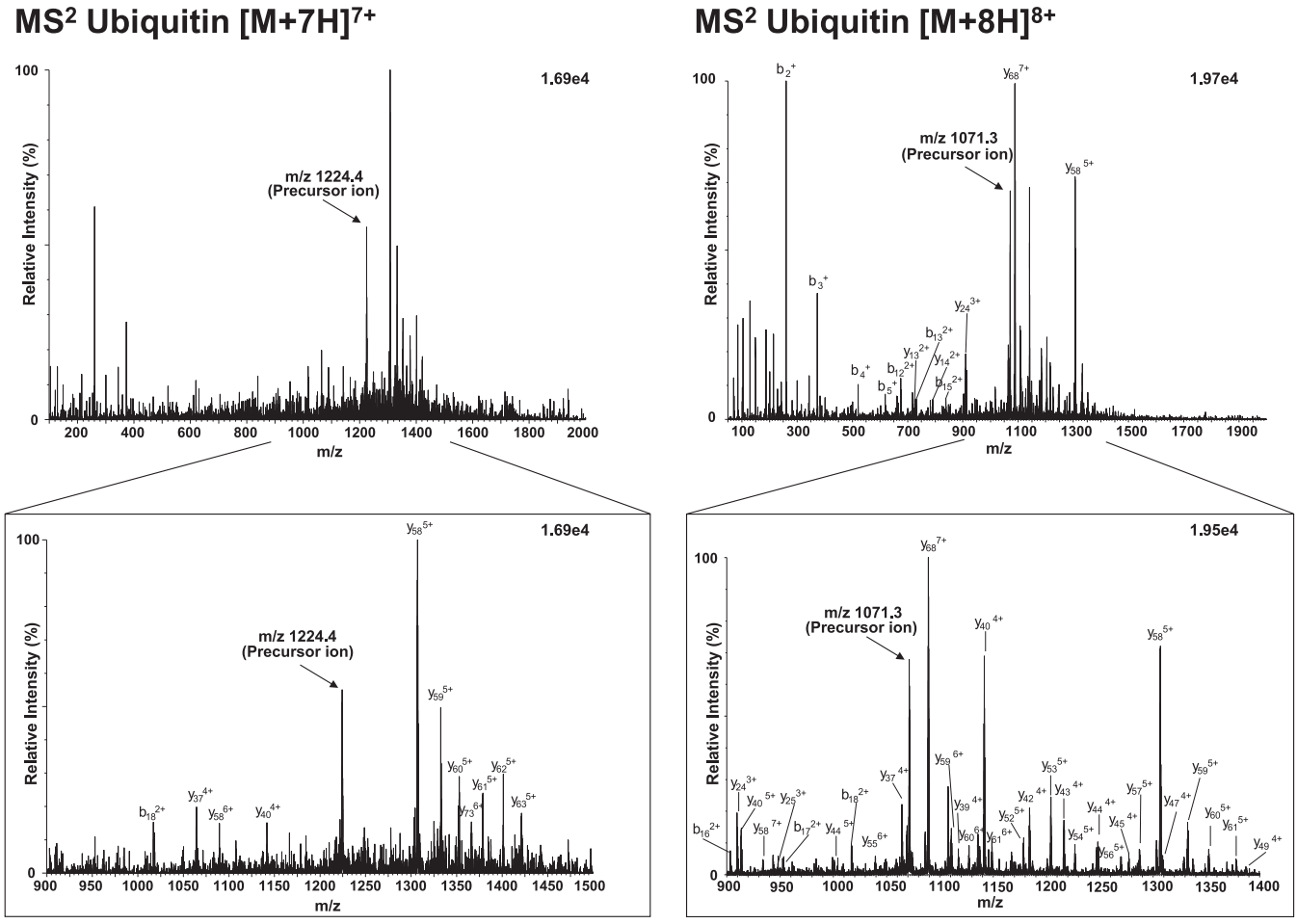

FIG. 4. **MS² spectrum of the precursor ion [M+7H]$^{7+}$ (*m/z* 1224.4) and [M+8H]^{8} (m/z 1071.3) of bovine ubiquitin recorded in real-time in positive mode using the SpiderMass prototype.** 2 μl of analyte at 5×10^{-4} M was deposited onto a glass slide and submitted to 5s laser irradiation period (ca. 50 laser shots).

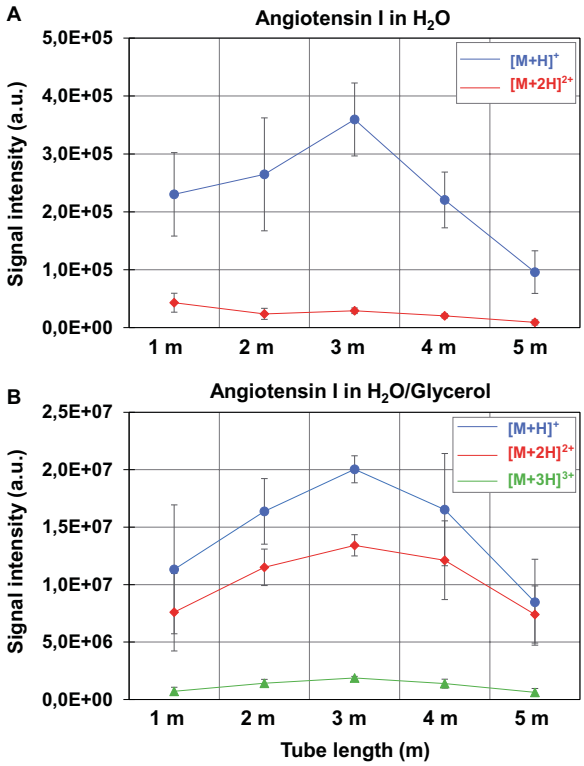

FIG. 5. **Evolution of the MS signal intensity (peak area, a.u.) of the protonated signals (singly-, doubly- and triply-charged if observed) of angiotensin I at varying transfer tube lengths.** Water and glycerol/water (1:1, v/v) were used as matrix. Tube lengths of 0.01, 1, 2, 3, and 5 m were tested. 2 μl of analyte at 5×10^{-4} M was deposited onto a glass slide and submitted to 5s laser irradiation period (ca. 50 laser shots).

if the ions are already formed in the early phase of the desorption process, or later during their transfer to the MS instrument, or if the charge state distribution is affected by the long transfer. This was investigated by setting transfer tubes of different lengths ranging from 10 cm to 5 m onto the instrument. Evolution of the ion signals observed in the MS spectra is presented in Fig. 5 for angiotensin I with water and glycerol/water as matrix and in supplemental Fig. S10 for ubiquitin in glycerol/water. First and very importantly, signals of the two analytes were observed in all tested conditions, which means that ions survive over 5 m of transfer by simple aspiration in a plastic tubing. Looking more in detail, the evolution of the signal intensity shows an important decrease only when a 5 m transfer tube is used, although the signal-to-noise ratio remains good (supplemental Fig. S11–S13). Very surprisingly the highest intensity was not always obtained using the shortest tubes. On average, 3 m was the tube length for which the highest reproducibility was reached, with total signal intensity rather like that using 10 cm or even longer tubes in the case of angiotensin I in glycerol/water (supplemental Fig. S12). In terms of charge state distribution no major modification was observed for the different tube lengths. This is particularly striking for ubiquitin (supplemental Fig. S13) because of the large charge state distribution. Thus, very interestingly the Remote IR-MALDI system can be placed 5 m apart from the instrument without major perturbation of performance or changes in the MS patterns. We also looked at the influence of the transfer tube temperature on the MS spectra by heating the transfer tube from 20 °C up to 80 °C using 2 m transfer tube. For angiotensin I in water, the intensity remains relatively stable up to 60 °C as well as the ratio of the doubly-charged to singly-charged protonated signals, but a strong signal decrease is observed at 80 °C (supplemental Fig. S14). In glycerol/water, a drastic decrease of the multiply charged ion signals was observed with increasing transfer tube temperature from RT to 80 °C while the intensity of the singly charge ion was almost constant (supplemental Fig. S15). This charge shift comes along with the progressive appearance of singly-charged sodium and potassium adducts which were absent at 20 °C. Thus, with heating the spectra obtained using glycerol/water become very similar to those obtained with pure water. For ubiquitin in glycerol/water (Fig. 6), this phenomenon is even more pronounced. Above 40 °C there is a total drop in intensity and no analyte signal is observed at 60 °C. Again, a clear shift of the charge state distribution toward the lower charge states is observed when comparing T = 20 °C and 40 °C. These results demonstrate a different behavior when water alone is used as matrix compared with glycerol/water mixture. For water, the temperature is only weakly affecting the signal except at higher temperature where it induces signal loss. For glycerol/water, the signal is clearly decreasing with temperature especially for higher molecular weight analytes, accompanied by a decrease in charge state.

The effect of pH of the solution on the charge state distribution was also investigated. The evolution of the MS spectra of ubiquitin in water and glycerol/water for pH ranging from 3 up to 9 are presented in Fig. 7. In water and above pH 5, no signal is observed for ubiquitin, whereas at lower pH (pH 3), the signal is largely decreased and with reduced sodium and potassium adducts. In glycerol/water, the signal is observed for all pH values. Again, the highest signal intensity is observed at pH 5. A shift of the charge state distribution toward lower charge along with a signal intensity decrease is observed above pH 5 which is more perceptible at pH 9. This is rather expected because of the reduction of protons in the solution. At pH 3, the signal intensity is lower than at pH 5 but very interestingly two charge state distributions are observed. The observation of these two charge states for ubiquitin indicates the co-existence of two conformations of the protein in solution which are kept during ion formation and detected in the MS spectrum. This is very similar to what is observed in conventional ESI. Several publications describe the observation of multiple conformations for certain proteins such as ubiquitin or cytochrome C in acidic conditions at pH close to 3 or below. It has also been demonstrated in different works

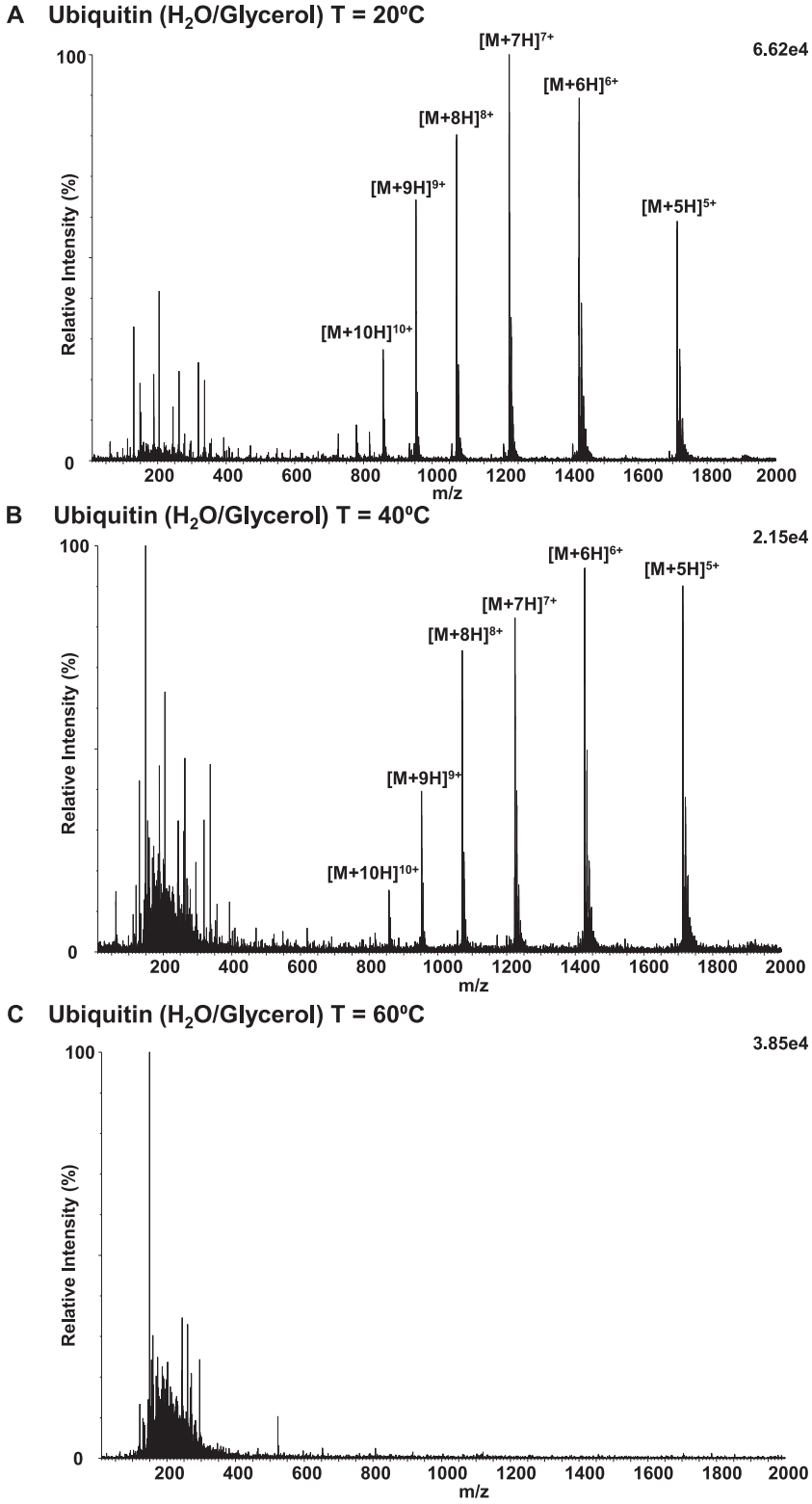

FIG. 6. **Evolution of the MS spectra of bovine ubiquitin with the temperature of the transfer tube (for 2 m transfer tube length).** Glycerol/water (1:1, v/v) was used as matrix. (*A*) T = 20 °C, (*B*) T = 40 °C and (*C*) T = 60 °C. Signals in the low *m/z* range [100–400] are attributed to pyrolysis products released by the heated coil at the interface of the mass spectrometer and are not coming from the analyte. 2 μl of analyte at 5×10^{-4} M was deposited onto a glass slide and submitted to 5s laser irradiation period (ca. 50 laser shots).

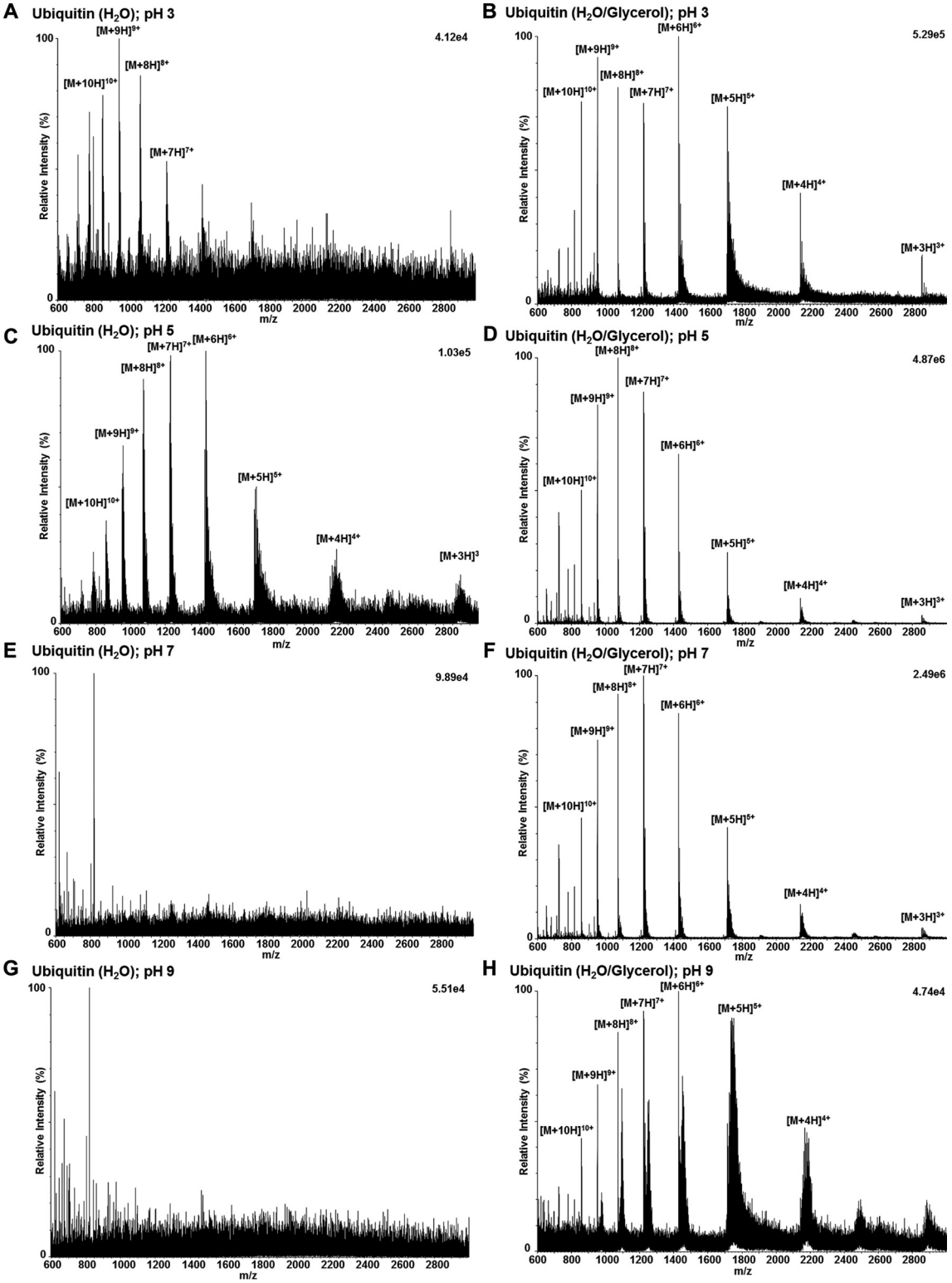

FIG. 7. **Evolution of the MS spectra of bovine ubiquitin as a function of solution pH, recorded using the Re-AP-IR-MALDI system in the positive mode and using water (*A*, *C*, *E*, *G*) or glycerol/water (1:1, v/v) (*B*, *D*, *F*, *H*) as matrix.** (*A*, *B*) pH 3, (*C*, *D*) pH 5, (*E*, *F*) pH 7, (*G*, *H*) pH 9. The transfer tube length was fixed at 3 m. 2 μl of analyte at 5×10^{-4} M was deposited onto a glass slide and submitted to 5s laser irradiation period (ca. 50 laser shots).

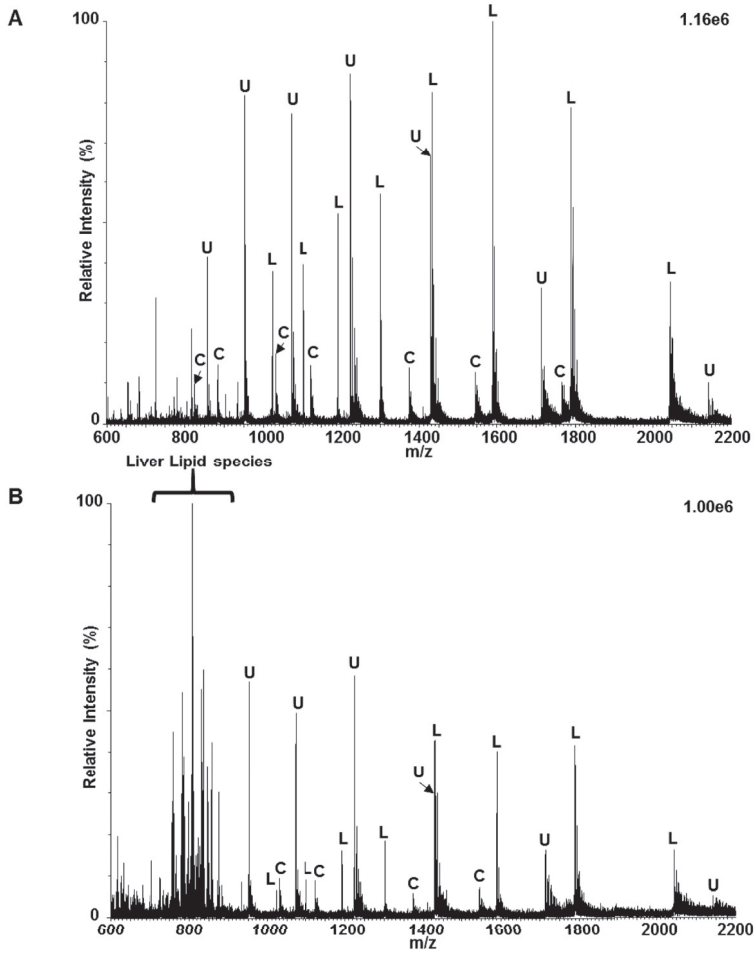

FIG. 8. **MS spectra recorded in positive mode using the Remote IR-MALDI system of a standard protein mix composed of bovine Insulin, bovine ubiquitin, cytochrome C, and myoglobin prepared in glycerol/water.** *A*, Solution is spotted onto a glass slide or, on a raw piece of bovine liver tissue. Analyses were conducted after complete absorption of the solution by the tissue. Spectrum shows the presence of both endogenous signals from the tissue (especially lipid signals in the lower *m/z* range) as well as the exogenous standard proteins. Samples was submitted to 5s laser irradiation periods (ca. 50 laser shots).

that glycerol stabilizes protein conformations (27, 28). Similar studies were also conducted on lysozyme and cytochrome C in glycerol/water (supplemental Fig. S16). Both lysozyme and cytochrome C showed behavior like ubiquitin. Again, the highest signal intensity was observed at pH 5 and at pH 3 cytochrome C showed a doubly-charged state distribution indicating the co-existence of two conformations of the protein in that condition.

Finally, we wanted to examine the behavior of proteins in a context closer to the one on tissue and not only in solution analyzing standards from droplets. Fig. 8 shows a comparison of the MS spectra recorded for the protein standard mix alone and spotted in glycerol/water on the sample plate or after deposition and adsorption onto a raw piece of model tissue (bovine liver). Interestingly, very similar charge state distributions were observed for the different proteins when analyzed after deposition on tissue. The main difference is the presence of intense signals in the lower m/z range corresponding to endogenous lipids, when the protein mix is spotted on the bovine liver section. The observed lipids are those expected when bovine liver is analyzed alone using the Remote IR MALDI SpiderMass system. This indicates that the observation of the charge state distribution is not only related to the initial solution condition of the analytes.

DISCUSSION

The Remote IR-MALDI (SpiderMass) system permits analysis of peptides and proteins and very interestingly obtained MS spectra are very similar to those that would be obtained using conventional ESI. Studying the influence of different parameters is necessary to get a better picture of the underlying fundamental mechanisms. An essential observation is the stability of signal intensity and charge state distribution with tube length. Surprisingly, many of these ions are not lost even after 5 m of transfer under AP conditions simply using the instrument vacuum to transport ions. This observation can

be supported by two different interpretations (1) a cluster model with the presence of charges at the early phase of the desorption process or (2) a late ion creation at the inlet of the MS instrument. For a long time, cluster desolvation has been postulated to explain certain features observed in conventional vacuum UV-MALDI (29, 30). Both the presence of analyte/matrix clusters (31, 32) and their difficult desolvation under conventional vacuum conditions have been demonstrated (33, 34). It was therefore hypothesized that MALDI probably generates highly charged ions, but that they are not observed in conventional configurations because of reneutralization processes or insufficient desolvation, considering thus ions as lucky survivors (35). In that view, ESI and MALDI mechanisms are very similar, with the matrix acting as a solvent. More recently, the various experimental configurations tested by Trimpin *et al.* (25) allowed the observation of highly charged state ions that support this view. However, it is still not completely rationalized why certain conditions allow for the observation of multiply charged ions.

In our Remote IR-MALDI system, ions are formed under AP conditions without any electric field either initially at the laser irradiation site, or later in the transfer tube. It should be noted that similar results were obtained using two other MS instruments with different interfaces and inlets (a) a 3D ion trap with an indirect heating of the transfer capillary (through heated N2, T = 400 °C), and (b) a Q-orbitrap with a directly heated transfer capillary (T = 250 °C). However, these instruments have different configurations rendering the comparison difficult. To better understand the phenomenon we experimented with the temperature of the heated khantal coil placed at the interface of our Q-TOF instrument. supplemental Fig. S17and S18 show the results for angiotensin I and cytochrome *c* when switching-off or heating up the heated coil by modulating the current intensity. When the heated coil is switched-off, the signal decreases by a factor 89 for angiotensin I and 4.7 for cytochrome *c* compared with I = 2.5 A (about T = 750 °C) but multiply charged ions are still observed even though the charge distribution is shifted toward lower charge states. For I = 4 A (T>1000 °C) the total signal intensity is increased compared with 2.5 A (respectively 2.4 and 2 folds higher for angiotensin I and cytochrome *c*) but the average charge state is very slightly decreased. This is most likely caused by the emission of electrons at high temperature which can lead to ions reneutralization. The observation of highly charged ions is therefore not related to a specific interface, inlet or instrument. These results finally support a cluster model where charges are already present from the very beginning and released by breaking down the clusters at the inlet of the instrument, with higher efficiency when a hot surface is used. The heated interface is beneficial to improve sensitivity by assisting with clusters desolvation or aggregation disruption but is not promoting the creation of charges on the clusters to our opinion. Many configurations were studied and developed over the past 15 years in MALDI; albeit rendering comparisons somehow difficult, these tend to show that higher charge states are apparently related to AP conditions (23, 24, 36, 37). It is commonly acknowledged that a heated transfer capillary has an important role to play in the observation of highly charged ions for those ions generated under AP because more charge states have been found when increasing the temperature of the transfer capillary. This was logically explained by the desolvation action of the temperature on the clusters. In our configuration the heated interface is clearly beneficial for the observation of multiply charged ions but is not mandatory. On the other hand, thinking of clusters of analyte/matrix and early ion formation, one would expect to observe changes within the charge state distribution for the different tube lengths tested because of cluster desolvation or by reneutralization because of collisions on the tube wall. However, this is not what is observed. It can be hypothesized that the global intensity increase for the 3 m tube length is related to a better desolvation of matrix/analyte clusters and that the slight decrease in signal intensity above 5 m would then be related to material lost because of lower efficiency of the transfer with respect to the turbulence flows in the tube. This would mean that our conditions provide a favorable environment for soft desolvation, preserving the initial charges. Moreover, increasing the temperature on the transfer line contributes to reducing the charge state when glycerol/water is used as matrix and can lead to a total extinction of the signal for highest temperatures. All these results suggest that a fine balance between cluster stabilization and desolvation must be found to preserve the highly charged ions (38). Also, we observe higher charge states when compared with conventional configurations, even when using pure water as matrix, which might suggest the importance of cluster stabilization at the early stages of desorption of their desolvation during the transfer in conditions avoiding their reneutralization. In this picture, the ion formation is seen very closely related to ion formation in ESI. The evolution of the charge state distribution with the pH of solution strengthens this hypothesis because what is observed is again very similar to ESI. Very strikingly the observation of the coexistence of protein conformations also is in favor of a very soft ionization mechanisms like in ESI allowing to preserve protein conformation. Finally, because protein standards are analyzed from solution, the translation to an ESI-like mechanism (Fig. 9) is relatively straightforward if one thinks that the laser can promote a pulsed droplet spraying system in place of electronebulization spray conditions. However, similar spectra are obtained when the protein standards are spotted and adsorbed onto a tissue piece. But, because we are promoting water excitation for desorption/ionization, and because we have observed that tissues clearly show characteristic dehydration after laser irradiation, it is very probable that water/analyte clusters similar to ESI charged droplets are generated.

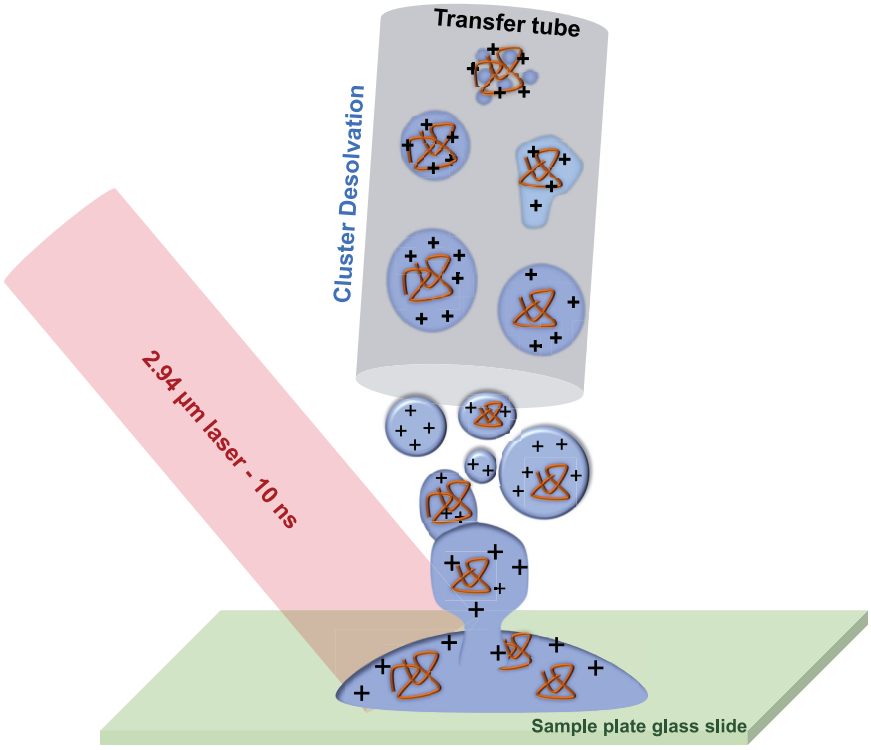

FIG. 9. **Schematic representation of desorption/ionization mechanism occurring in the Remote IR-MALDI (SpiderMass) system.**

CONCLUSION

We have demonstrated that peptides and proteins can be remotely analyzed in real-time up to 5 m using the Remote IR-MALDI system (SpiderMass) operating in mid-IR and atmospheric pressure without any post-ionization. Very interestingly, in this configuration high charge state ion distributions are promoted. Multiply charged ions were observed in pure water already but ion charged states were even increased by using 50% glycerol, glycerol having also the advantage to stabilize the system by preventing the sample from drying too fast. SpiderMass MS spectra contain peaks like those obtained by conventional ESI MS than using other conventional AP-MALDI sources. This is of high interest for the identification of proteins by Top-Down or Bottom-Up strategies. Higher charge states are known to be less stable and give higher fragmentation yields under conventional low CID or Post Source Decay (PSD) conditions which is often a difficulty in conventional vacuum UV-MALDI with respect to identification of peptides and proteins (39). The evolution of peptide and protein signals under different conditions including laser wavelength, transfer tube length and temperature suggests a cluster model with charges being present at the early stages of desorption/ionization process. The stability of the signal and charge state distribution for transfer tubes of 10 cm up to 5 m in length is interesting because the molecular patterns are not affected by the initial conditions nor by the system configuration. This offers great flexibility potentially improving versatility in applications because sampling can be performed remotely from the instrument. We also demonstrated that the desorption/ionization process is very soft allowing to maintain protein conformation as in ESI. This leads to a picture where the laser, by excitation of water, induces the desorption of water (or water/glycerol) clusters or droplets already containing highly charged analytes which then softly desolvate during their transport to the instrument in a mechanism extremely close to ESI. Observation of proteins and similar spectral features on tissue, when protein standards are deposited on raw tissue pieces, could potentially open the way to their direct analysis from biological samples. Thus, we expect the applicability of this instrument in the near future in the analysis of raw samples even in the *in vivo* context, providing new insight to proteomics by allowing for a progressive transition to *in vivo* real-time proteomics.

DATA AVAILABILITY

The data files used for analysis were deposited at the ProteomeXchange Consortium (17) (http://proteomecentral.proteomexchange.org) via the PRIDE partner repository (18) with the project accession: PXD008092.

* This work was supported by grants from Inserm PhysiCancer (project SPIDERMASS, Prof. M. Salzet), ANR Santé Bien-être (Project Reality'MS, Prof. I. Fournier) and SATT Nord (Maturation Program, Prof. I. Fournier and P. Saudemont). Also funded by SIRIC ONCOLille (Prof. I. Founier) Grant INCa-DGOS-Inserm 6041.

[S] This article contains supplemental material.

‖ To whom correspondence should be addressed: Laboratoire Protéomique, Réponse Inflammatoire et Spectrométrie de Masse

(PRISM) - Inserm U1192 - Université de Lille, Bât SN3, 1er étage, Cité Scientifique, F-59655 Villeneuve d'Ascq Cedex, France. Tel.: +33-(0)3-20-43-41-94; Fax: +33-(0)3-20-43-40-54; E-mail: isabelle.fournier@univ-lille.fr.

Author contributions: I.F., M.Z., and M.S. conceived the study. BF and PS performed the experiments. I.F., M.S., and M.Z. supervised the project, and participated in experimental design and data analyses. J.Q., I.F., and M.S. participated in the writing of the manuscript with contributions coming from all co-authors. I.F., M.S., C.F., and M.Z. also obtained funds for the project.

REFERENCES

1. Huang, M. Z., Cheng, S. C., Cho, Y. T., and Shiea, J. (2011) Ambient ionization mass spectrometry: a tutorial. *Anal. Chim. Acta* **702,** 1–15
2. Harris, G. A., Galhena, A. S., and Fernandez, F. M. (2011) Ambient sampling/ionization mass spectrometry: applications and current trends. *Anal. Chem.* **83,** 4508–4538
3. Alberici, R. M., Simas, R. C., Sanvido, G. B., Romão, W., Lalli, P. M., Benassi, M., Cunha, I. B., and Eberlin, M. N. (2010) Ambient mass spectrometry: bringing MS into the "real world". *Anal. Bioanal. Chem.* **398,** 265–294
4. Wu, C., Dill, A. L., Eberlin, L. S., Cooks, R. G., and Ifa, D. R. (2013) Mass spectrometry imaging under ambient conditions. *Mass Spectrometry Rev.* **32,** 218–243
5. Ferreira, C. R., Yannell, K. E., Jarmusch, A. K., Pirro, V., Ouyang, Z., and Cooks, R. G. (2016) Ambient ionization mass spectrometry for point-of-care diagnostics and other clinical measurements. *Clin. Chem.* **62,** 99–110
6. Gross, J. H. (2014) Direct analysis in real time–a critical review on DART-MS. *Anal. Bioanal. Chem.* **406,** 63–80
7. Cody, R. B., Laramee, J. A., and Durst, H. D. (2005) Versatile new ion source for the analysis of materials in open air under ambient conditions. *Anal. Chem.* **77,** 2297–2302
8. Zhang, J. I., Costa, A. B., Tao, W. A., and Cooks, R. G. (2011) Direct detection of fatty acid ethyl esters using low temperature plasma (LTP) ambient ionization mass spectrometry for rapid bacterial differentiation. *Analyst* **136,** 3091–3097
9. Liu, Y., Lin, Z., Zhang, S., Yang, C., and Zhang, X. (2009) Rapid screening of active ingredients in drugs by mass spectrometry with low-temperature plasma probe. *Anal. Bioanal. Chem.* **395,** 591–599
10. Laiko, V. V., Moyer, S. C., and Cotter, R. J. (2000) Atmospheric pressure MALDI/ion trap mass spectrometry. *Anal. Chem.* **72,** 5239–5243
11. Fatou, B., Wisztorski, M., Focsa, C., Salzet, M., Ziskind, M., and Fournier, I. (2015) Substrate-mediated laser ablation under ambient conditions for spatially-resolved tissue proteomics. *Sci. Reports* **5,** 18135
12. Balog, J., Szaniszlo, T., Schaefer, K.-C., Denes, J., Lopata, A., Godorhazy, L., Szalay, D., Balogh, L., Sasi-Szabo, L., Toth, M., and Takats, Z. (2010) Identification of biological tissues by rapid evaporative ionization mass spectrometry. *Anal. Chem.* **82**, 7343–7350
13. Balog, J., Sasi-Szabo, L., Kinross, J., Lewis, M. R., Muirhead, L. J., Veselkov, K., Mirnezami, R., Dezso, B., Damjanovich, L., Darzi, A., Nicholson, J. K., and Takats, Z. (2013) Intraoperative tissue identification using rapid evaporative ionization mass spectrometry. *Sci. Transl. Med.* **5,** 194ra193
14. Fatou, B., Saudemont, P., Leblanc, E., Vinatier, D., Mesdag, V., Wisztorski, M., Focsa, C., Salzet, M., Ziskind, M., and Fournier, I. (2016) In vivo real-time mass spectrometry for guided surgery application. *Sci. Reports* **6,** 25919
15. Balog, J., Kumar, S., Alexander, J., Golf, O., Huang, J., Wiggins, T., Abbassi-Ghadi, N., Enyedi, A., Kacska, S., Kinross, J., Hanna, G. B., Nicholson, J. K., and Takats, Z. (2015) In vivo endoscopic tissue identification by rapid evaporative ionization mass spectrometry (REIMS). *Angew Chem Int Ed Engl* **54,** 11059–11062
16. Niedermeyer, T. H., and Strohalm, M. (2012) mMass as a software tool for the annotation of cyclic peptide tandem mass spectra. *PLoS ONE* **7,** e44913
17. Vizcaino, J. A., Deutsch, E. W., Wang, R., Csordas, A., Reisinger, F., Rios, D., Dianes, J. A., Sun, Z., Farrah, T., Bandeira, N., Binz, P. A., Xenarios, I., Eisenacher, M., Mayer, G., Gatto, L., Campos, A., Chalkley, R. J., Kraus, H. J., Albar, J. P., Martinez-Bartolome, S., Apweiler, R., Omenn, G. S., Martens, L., Jones, A. R., and Hermjakob, H. (2014) ProteomeXchange provides globally coordinated proteomics data submission and dissemination. *Nat. Biotechnol.* **32,** 223–226
18. Vizcaino, J. A., Cote, R. G., Csordas, A., Dianes, J. A., Fabregat, A., Foster, J. M., Griss, J., Alpi, E., Birim, M., Contell, J., O'Kelly, G., Schoenegger, A., Ovelleiro, D., Perez-Riverol, Y., Reisinger, F., Rios, D., Wang, R., and Hermjakob, H. (2013) The PRoteomics IDEntifications (PRIDE) database and associated tools: status in 2013. *Nucleic Acids Res.* **41,** D1063–D1069
19. Talrose, V. L., Person, M. D., Whittal, R. M., Walls, F. C., Burlingame, A. L., and Baldwin, M. A. (1999) Insight into absorption of radiation/energy transfer in infrared matrix-assisted laser desorption/ionization: the roles of matrices, water and metal substrates. *Rapid Commun. Mass Spectrom.* **13,** 2191–2198
20. Overberg, A., Karas, M., Bahr, U., Kaufmann, R., and Hillenkamp, F. (1990) Matrix-assisted infrared-laser (2.94 μm) desorption/ionization mass spectrometry of large biomolecules. *Rapid Commun. Mass Spectrom.* **4,** 293–296
21. Overberg, A., Karas, M., Hillenkamp, F., and Cotter, R. (1991) Matrix-assisted laser desorption of large biomolecules with a TEA-CO2-laser. *Rapid Commun. Mass Spectrom.* **5,** 128–131
22. Nordhoff, E., Ingendoh, A., Cramer, R., Overberg, A., Stahl, B., Karas, M., Hillenkamp, F., Crain, P., and Chait, B. (1992) Matrix-assisted laser desorption/ionization mass spectrometry of nucleic acids with wavelengths in the ultraviolet and infrared. *Rapid Commun. Mass Spectrom.* **6,** 771–776
23. Laiko, V. V., Taranenko, N. I., Berkout, V. D., Yakshin, M. A., Prasad, C. R., Lee, H. S., and Doroshenko, V. M. (2002) Desorption/ionization of biomolecules from aqueous solutions at atmospheric pressure using an infrared laser at 3 microm. *J. Am. Soc. Mass Spectrom.* **13,** 354–361
24. König, S., Kollas, O., and Dreisewerd, K. (2007) Generation of highly charged peptide and protein ions by atmospheric pressure matrix-assisted infrared laser desorption/ionization ion trap mass spectrometry. *Anal. Chem.* **79,** 5484–5488
25. Trimpin, S. (2016) "Magic" Ionization Mass Spectrometry. *J. Am. Soc. Mass Spectrom.* **27,** 4–21
26. Soltwisch, J., Jaskolla, T. W., Hillenkamp, F., Karas, M., and Dreisewerd, K. (2012) Ion yields in UV-MALDI mass spectrometry as a function of excitation laser wavelength and optical and physico-chemical properties of classical and halogen-substituted MALDI matrixes. *Anal. Chem.* **84,** 6567–6576
27. Konermann, L., and Douglas, D. (1998) Equilibrium unfolding of proteins monitored by electrospray ionization mass spectrometry: distinguishing two-state from multi-state transitions. *Rapid Commun. Mass Spectrom.* **12,** 435–442
28. Grandori, R., Matecko, I., Mayr, P., and Müller, N. (2001) Probing protein stabilization by glycerol using electrospray mass spectrometry. *J. Mass Spectrom.* **36,** 918–922
29. Karas, M., and Krüger, R. (2003) Ion formation in MALDI: the cluster ionization mechanism. *Chem. Rev.* **103,** 427–440
30. Jaskolla, T. W., and Karas, M. (2011) Compelling evidence for lucky survivor and gas phase protonation: the unified MALDI analyte protonation mechanism. *J. Am. Soc. Mass Spectrom.* **22,** 976–988
31. Fournier, I., Brunot, A., Tabet, J., and Bolbach, G. (2005) Delayed extraction experiments using a repulsing potential before ion extraction: evidence of non-covalent clusters as ion precursor in UV matrix-assisted laser desorption/ionization. Part II—Dynamic effects with α-cyano-4-hydroxycinnamic acid matrix. *J. Mass Spectrom.* **40,** 50–59
32. Fournier, I., Brunot, A., Tabet, J., and Bolbach, G. (2002) Delayed extraction experiments using a repulsive potential before ion extraction: evidence of clusters as ion precursors in UV-MALDI. Part I: dynamical effects with the matrix 2, 5-dihydroxybenzoic acid. *Int. J. Mass Spectrom.* **213,** 203–215
33. Krutchinsky, A. N., and Chait, B. T. (2002) On the nature of the chemical noise in MALDI mass spectra. *J. Am. Soc. Mass Spectrom***13,** 129–134
34. Sachon, E., Clodic, G., Blasco, T., and Bolbach, G. (2007) Protein desolvation in UV matrix-assisted laser desorption/ionization (MALDI). *J. Am. Soc. Mass Spectrom* **18,** 1880–1890
35. Karas, M., Glückmann, M., and Schäfer, J. (2000) Ionization in matrix-

assisted laser desorption/ionization: singly charged molecular ions are the lucky survivors. *J. Mass Spectrom.* **35,** 1–12
36. Dreisewerd, K. (2014) Recent methodological advances in MALDI mass spectrometry. *Anal. Bioanal. Chem.* **406,** 2261–2278
37. Cramer, R., Pirkl, A., Hillenkamp, F., and Dreisewerd, K. (2013) Liquid AP-UV-MALDI Enables Stable Ion Yields of Multiply Charged Peptide and Protein Ions for Sensitive Analysis by Mass Spectrometry. *Angewandte Chemie Int. Ed.* **52,** 2364–2367
38. Ryumin, P., Brown, J., Morris, M., and Cramer, R. (2016) Investigation and optimization of parameters affecting the multiply charged ion yield in AP-MALDI MS. *Methods* **104,** 11–20
39. Ryumin, P., Brown, J., Morris, M., and Cramer, R. (2017) Protein identification using a nanoUHPLC-AP-MALDI MS/MS workflow with CID of multiply charged proteolytic peptides. *Int. J. Mass Spectrom.* **416,** 20–28